The second parameter regime of the viscosity for quasi-steady state of sawtooth in Tokamaks

W. Zhang[1,2], Z. W. Ma[1,a)], H. W. Zhang[1], and X. Wang[1]

[1]Institute for Fusion Theory and Simulation, Department of Physics, Zhejiang University, Hangzhou 310027, China

[2]Princeton Plasma Physics Laboratory, P.O. Box 451, Princeton, New Jersey 08543, USA

Abstract:

The influence of the viscosity and the plasma beta on dynamics of sawtooth oscillations in Tokamaks is systematically conducted with the three-dimensional, toroidal, and compressible MHD code CLT. It is found that there are two parameter regimes of the viscosity for achieving a steady-state. With sufficiently high or low viscosity, the system eventually evolves into a steady-state. In the intermediate regime of the viscosity, the sawtooth exhibits a normal sawtooth oscillation. Since present Tokamaks operate in the very low viscosity regime, the quasi-steady state in the low viscosity and high plasma beta is more relevant to experimental conditions. In the steady-state, the mode structure is non-axisymmetric with the m/n=1/1 helicity, and the safety factor in the core becomes flattened, which may be related to the stationary state observed in DIII-D and some other Tokamaks. This finding of the steady-state in the low viscosity and high plasma beta regime might be helpful for future ITER steady-state operations.

a) Corresponding Author: zwma@zju.edu.cn

I. Introduction

Sawtooth is a periodic relaxation of the core plasma temperature. It is a common phenomenon for the magnetic confinement fusion device, whose central safety factor falls below one. [1-6] There are at least three different kinds of sawtooth oscillations, i.e., normal sawtooth, [1, 7] small sawtooth, [8] and compound sawtooth. [9] The normal sawtooth is dangerous for Tokamak operations as it can not only flatten center plasma temperature but also trigger neo-classical tearing modes in nearby resonant surfaces. [10-12]. It results in a significant reduction of energy confinement. However, the small sawtooth is less likely to trigger neo-classical tearing modes [13], and the temperature reduction caused by the small sawtooth crash is tolerable for the fusion reactor. [14] Besides, the small sawtooth is beneficial in preventing impurity accumulation in the core region. Consequently, a sawtooth crash with a small amplitude has been adopted in future fusion reactors. [15]

It is widely known that sawtooth behavior closely relates to the heating power of Tokamaks. In early small Tokamaks, the heating power is mainly from Ohm heating, and the sawtooth occurred in such Tokamaks is the normal sawtooth. [1] In advanced Tokamaks, there are many auxiliary heating methods, such as ion cyclotron resonance heating (ICRH), neutral beam injection (NBI), electron cyclotron resonance heating (ECRH), and lower hybrid current drive (LHCD). [6, 16-25] With additional heating power, the sawtooth period can be quite different from that, in which Ohm heating is dominant. One approach to control the sawtooth is intentionally decreasing the sawtooth period to achieve the small sawtooth or even a stationary state through additional heating. [26]

Due to the importance of sawtooth control, efforts have been made to investigate small-amplitude sawtooth and steady-state of sawtooth. [26-43] But the mechanism of the steady-state is still not clear, and it is worthy of studying further. A systematical simulation study with different plasma beta and viscosities is carried out to investigate the dynamics of sawtooth oscillations. It is found that a normal sawtooth oscillation takes place only in the intermediate parameter regime of the viscosity. With a

relatively high or low viscosity, the sawtooth oscillation quickly evolves into the small sawtooth or steady-state. In the low viscosity regime, the steady-state mainly results from the balance between the magnetic flux pumped by the dynamo effect and the flux carried away by non-axisymmetric plasma flow. It is also found that the intermediate regime of the viscosity becomes border with decreasing the thermal plasma beta.

In present experiments with a higher plasma beta and a lower viscosity (such as DIII-D[26], MAST[44], JET[37] and JT-60U[45]), it is more likely to achieve the steady-state with low viscosity. In the steady-state, the non-axisymmetric mode structure in the core region has the *m/n=1/1* helicity, and with $q \simeq 1$ in the core region, which is also consistent with that observed in DIII-D.[26]

II. Model description

In dimensionless units, the compressible resistive MHD equations used in CLT[46-49] is given as follows:

$$\frac{\partial \rho}{\partial t} = -\nabla \cdot (\rho \mathbf{v}) + \nabla \cdot [D \nabla (\rho)] \quad ,(1)$$

$$\frac{\partial p}{\partial t} = -\mathbf{v} \cdot \nabla p - \Gamma p \nabla \cdot \mathbf{v} + \nabla \cdot [\kappa_{\perp} \nabla (p - p_0)] + \nabla \cdot [\kappa_{\parallel} \nabla_{\parallel} p] \quad ,(2)$$

$$\frac{\partial \mathbf{v}}{\partial t} = -\mathbf{v} \cdot \nabla \mathbf{v} + (\mathbf{J} \times \mathbf{B} - \nabla p) / \rho + \nabla \cdot [\upsilon \nabla (\mathbf{v})] \quad ,(3)$$

$$\frac{\partial \mathbf{B}}{\partial t} = -\nabla \times \mathbf{E} \quad ,(4)$$

$$\mathbf{E} = -\mathbf{v} \times \mathbf{B} + \eta (\mathbf{J} - \mathbf{J}_0) \quad ,(5)$$

$$\mathbf{J} = \nabla \times \mathbf{B} \quad ,(6)$$

where ρ, p, $\mathbf{v}$, $\mathbf{B}$, $\mathbf{E}$, and $\mathbf{J}$ denote the plasma density, the plasma pressure, the electron pressure, the velocity, the magnetic field, the electric field, and the current density, respectively. The subscript “0” denotes the initial equilibrium quantities. $\Gamma (= 5/3)$ is the ratio of specific heat of plasma. η, D, $\kappa_{\perp}$, $\kappa_{\parallel}$, and υ are resistivity, diffusion coefficient, perpendicular and parallel thermal conductivity, and viscosity,

respectively. The variables are normalized as follows: $\mathbf{B}/B_0 \to \mathbf{B}$, $\mathbf{x}/a \to \mathbf{x}$, $\rho/\rho_0 \to \rho$, $\mathbf{v}/v_A \to \mathbf{v}$, $t/t_A \to t$, $p/(B_0^2/\mu_0) \to p$, $\mathbf{J}/(B_0/\mu_0 a) \to \mathbf{J}$, and $\mathbf{E}/(v_A B_0) \to \mathbf{E}$, where a is the minor radius, $v_A = B_0/\sqrt{\mu_0 \rho_0}$ is the Alfvén speed, and $t_A = a/v_A$ is the Alfvén time. B_0 and ρ_0 are the initial magnetic field and plasma density at the magnetic axis, respectively. The resistivity η, the diffusion coefficient D, the perpendicular and parallel thermal conductivity $\kappa_\perp$ and $\kappa_\parallel$, and the viscosity υ are normalized as follows: $\eta/(\mu_0 a^2/t_A) \to \eta$, $D/(a^2/t_A) \to D$, $\kappa_\perp/(a^2/t_A) \to \kappa_\perp$, $\kappa_\parallel/(a^2/t_A) \to \kappa_\parallel$, and $\upsilon/(a^2/t_A) \to \upsilon$, respectively**.** In CLT, $\eta(\mathbf{J}-\mathbf{J}_0)$ in eq. (5) acts as the magnetic pump [26] to recover the magnetic flux and produce periodic sawtooth oscillations.

III. Simulation results

A. Sawtooth oscillations with High β

A toroidal Tokamak configuration with aspect ratio $R_0/a = 4/1$ is chosen in our simulations. The initial *q* and pressure profiles are shown in Figure 1. The most unstable mode in the system is the *m/n*=1/1 resistive kink mode instability, where *m* and *n* are the poloidal and toroidal mode numbers, respectively. The initial equilibrium is obtained from the NOVA code. [50] The grids used in the present paper are $256\times32\times256$ (R,ϕ,Z). The convergence of the code has been ensured by varying both the resolutions of time and space. In this subsection, we carry out different viscosities: ν_0=1.0×10^{-3}, ν_0=1.0×10^{-4}, ν_0=2.0×10^{-5}, and ν_0=6.0×10^{-6} to investigate how the viscosity plays role on dynamics of sawtooth oscillations with high plasma beta, $\beta \sim 3.8\%$. The resistivity $\eta = 2.5\times10^{-6}$ is chosen only for saving computational time. Other parameters are chosen to be $D = 1.0\times10^{-4}$, $\kappa_\perp = 2.0\times10^{-5}$, and $\kappa_\parallel = 5\times10^{-2}$.

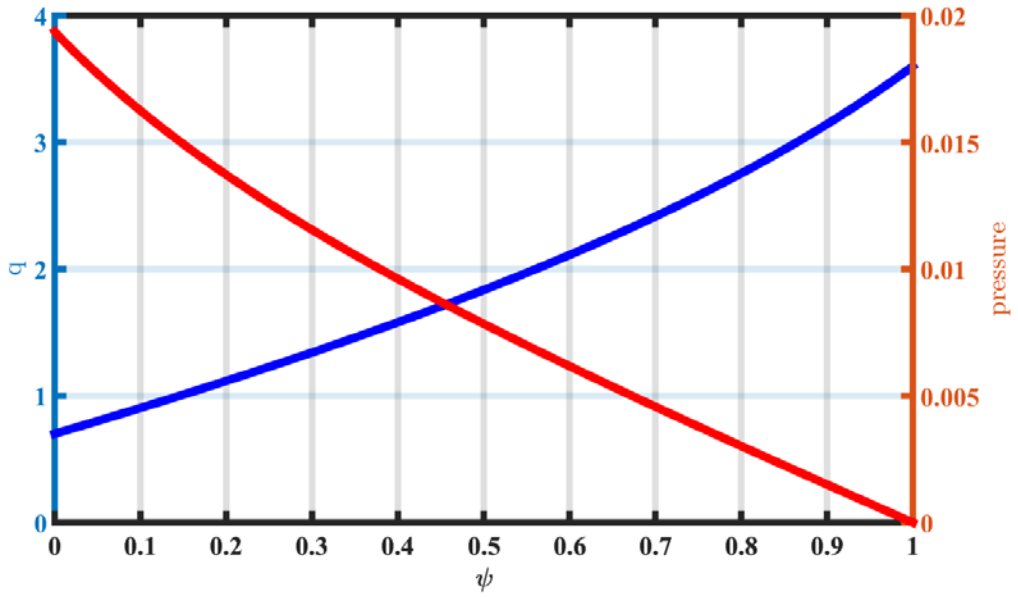

Figure 1 Initial safety factor q and pressure profiles.

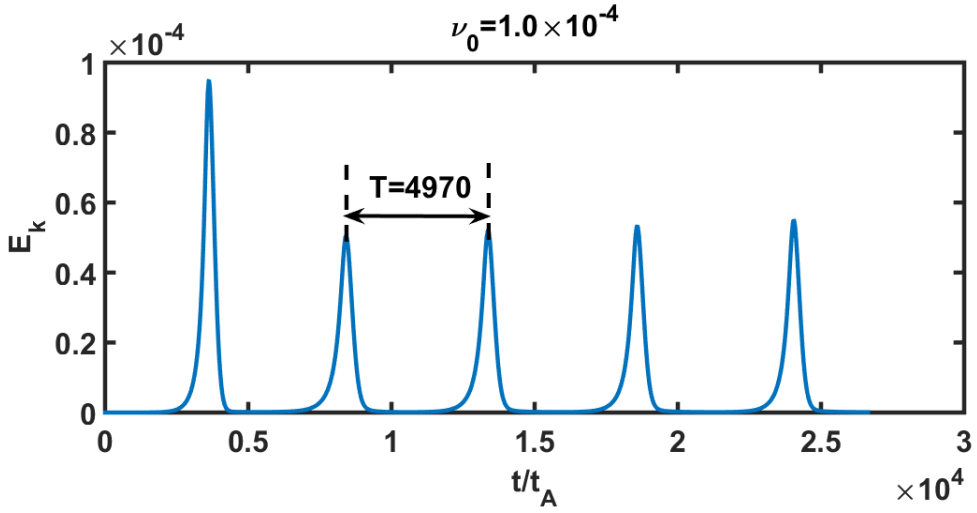

Figure 2 Evolution of the kinetic energy with $\nu_0=1.0\times10^{-4}$. The period of the normal sawtooth oscillation is $T\sim4970t_A$.

The evolution of kinetic energy for the case with $\nu_0=1.0\times10^{-4}$ is shown in Figure 2. As we can see, the oscillation exhibits the normal sawtooth oscillation with

the period T~4970t_A. The evolution of the plasma pressure profile along Z=0 and $\varphi = 0$ is shown in Figure 3. The pressure profile also exhibits periodic oscillations with the period T~4970t_A. Since the normal sawtooth has been intensively investigated in past decades, [51, 52] we will not discuss the normal sawtooth in detail in the present paper.

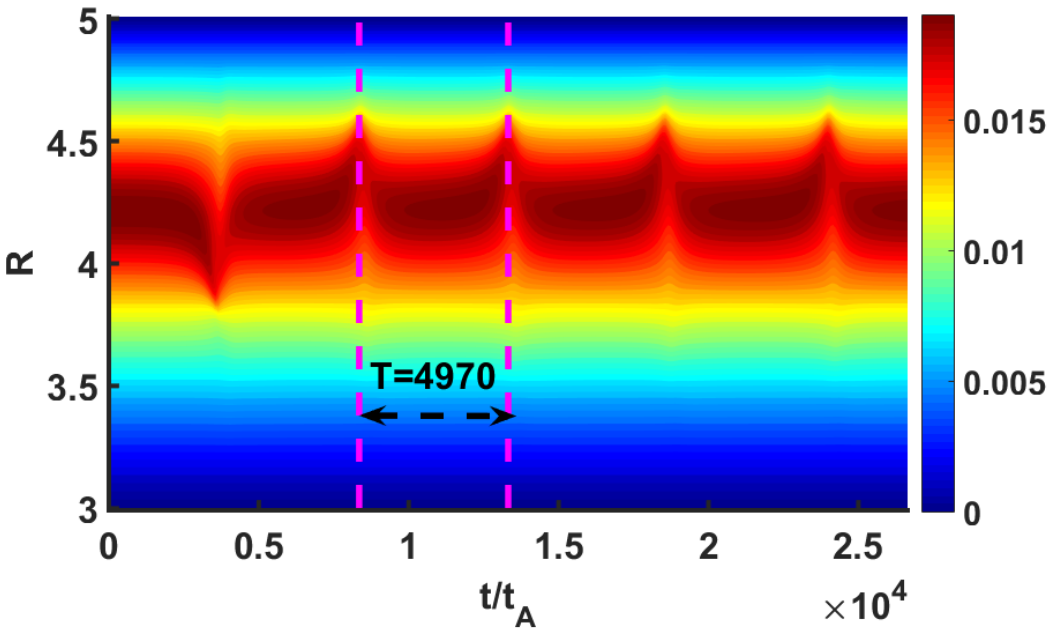

Figure 3 Evolution of the plasma pressure profile along Z=0 and $\varphi = 0$. The pressure profile exhibits periodic oscillations with the period T~4970t_A.

However, with lower viscosity, the sawtooth could turn into a small sawtooth oscillation. The evolutions of the kinetic energy and the pressure profile for the case with ν_0=2.0×10^{-5} are shown in Figures 4 and 5, respectively. It indicates that the period of the small sawtooth oscillations is reduced to T~1300t_A. The pressure of the hot core is much lower during the small sawtooth than the normal sawtooth, which suggests that, after the first massive pressure crash, the system is never fully recovered during the small sawtooth (Figure 5) while it is almost fully recovered during the normal sawtooth (Figure 3). Such kind of behavior could also be seen from the Poincare plots of magnetic fields (Figure 6 a and b). During the small

sawtooth, the *m/n*=1/1 magnetic island does not fill up the whole mixed region, while, it does in the normal sawtooth. During the small sawtooth oscillations, the island only periodically increases and decreases.

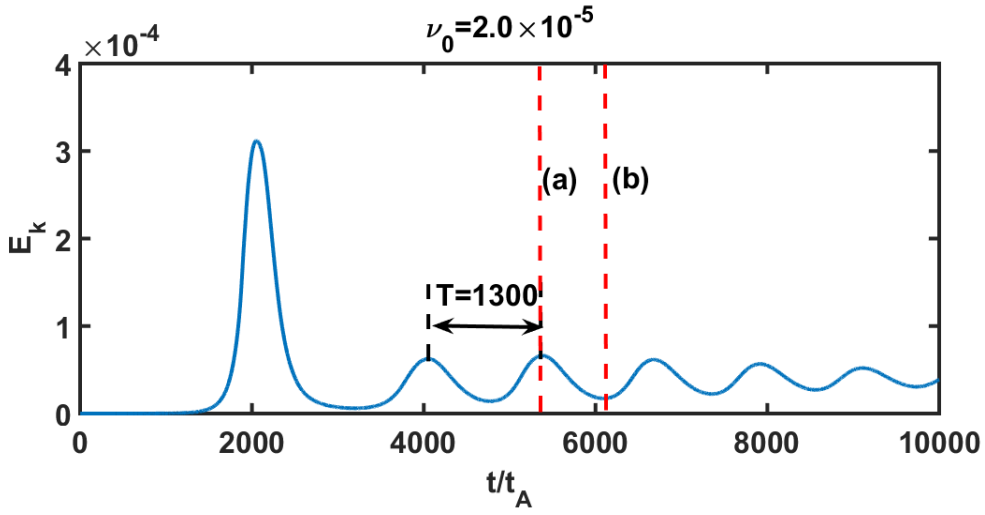

Figure 4 Evolution of the kinetic energy with ν_0=2.0×10^{-5}. The sawtooth shows small oscillations with a shorter period T~1300t$_A$. The peak time (a) $t = 5328t_A$ and the end time (b) $t = 6127t_A$ of the third cycle are labeled with vertical red dash lines.

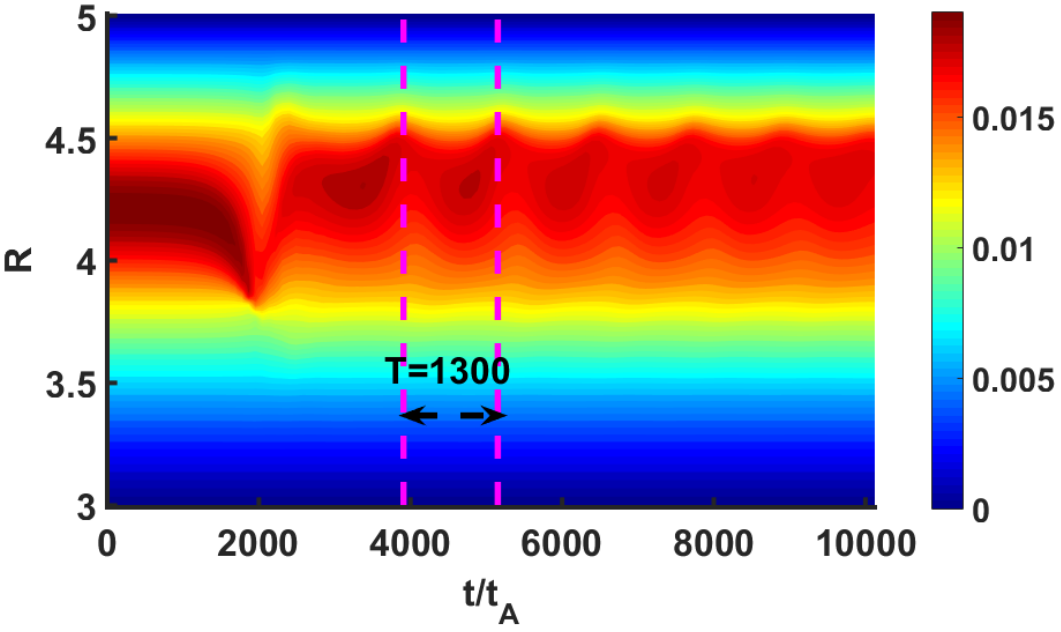

Figure 5 Evolution of the pressure profile at Z=0 with ν_0=2.0×10^{-5}. It is clear that, after the first crash, the pressure of the hot core is much lower for the small sawtooth

than for the normal sawtooth, which suggests that the system is not able to fully recover during the small sawtooth.

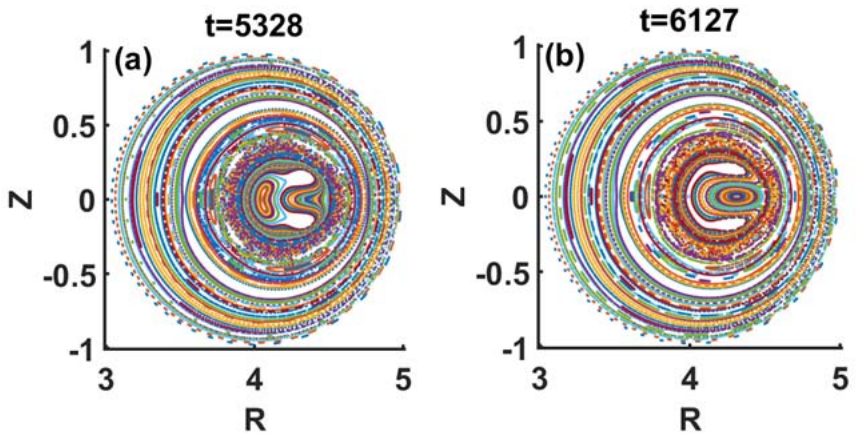

Figure 6 Poincare plots of magnetic fields at (a) $t = 5328t_A$ and (b) $t = 6127t_A$ for the small sawtooth. The *m/n*=1/1 magnetic island is not fully developed as it does in the normal sawtooth oscillation.

With sufficiently low viscosity $\nu_0 = 6.0 \times 10^{-6}$, the system evolves into a steady-state. As shown in Figure 7 and Figure 8, the kinetic energy and the pressure profile almost remain unchanged after $t = 6000t_A$, which means that the system could self-consistently evolve into the steady-state. The Poincare plots in the steady-state are shown in Figure 9. In the final stage, the *m/n*=1/1 magnetic island occupies a large region, and the system reaches the steady-state with non-asymmetric magnetic field, which is similar to the hybrid scenario which is often observed in many experiments. [26, 35, 44, 45, 53, 54] The small sawtooth and steady-state presented in the paper are similar to the results from M3D-C1.[27, 28]

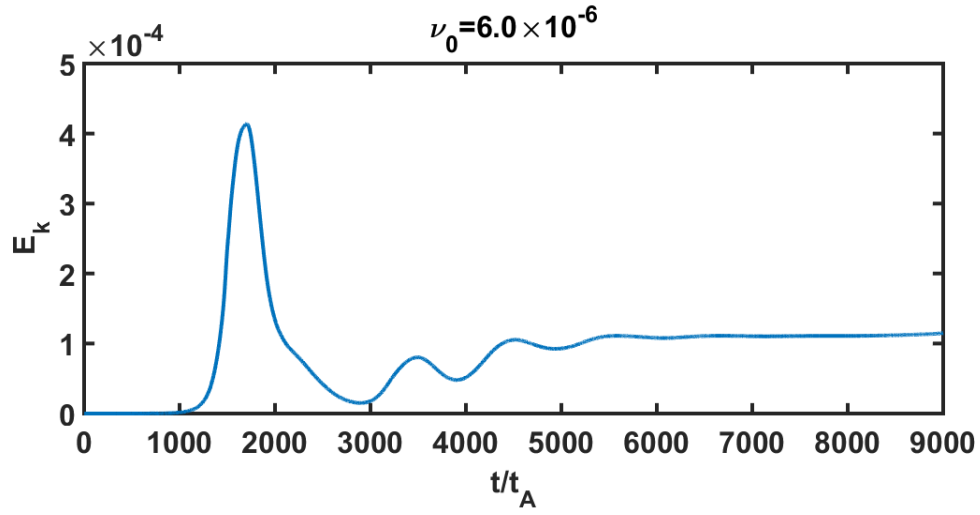

Figure 7 Evolution of kinetic energy of the case with ν_0=6.0×10^{-6}. After the first crash, the system evolves into a stationary state, and the kinetic energy almost remains unchanged after $t = 6000t_A$.

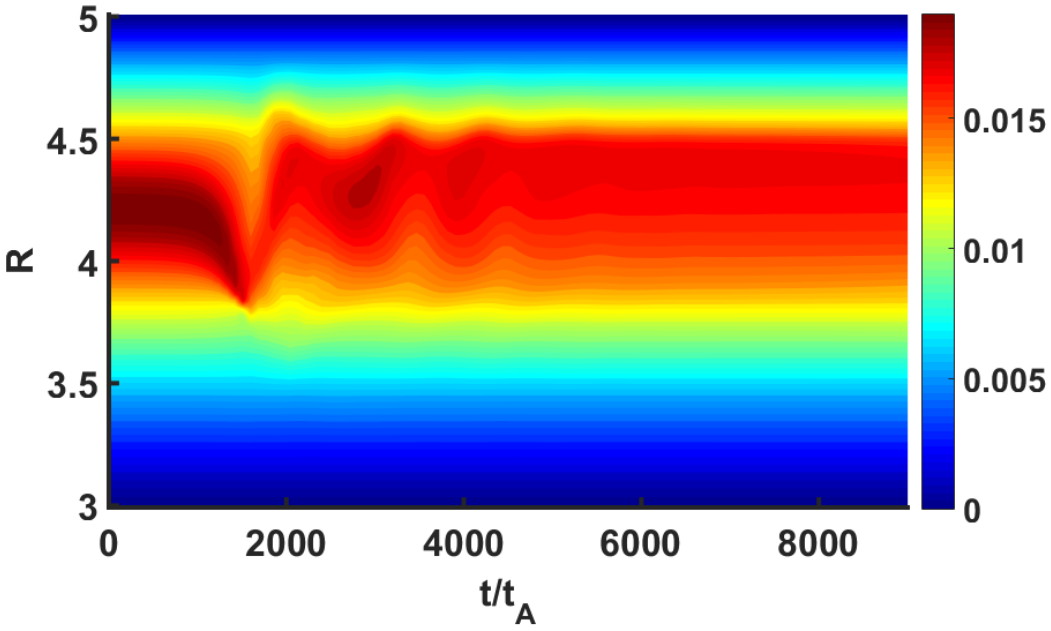

Figure 8 Evolution of pressure profile at Z=0 with ν_0=6.0×10^{-6}. After $t = 6000t_A$, the pressure profile almost remains unchanged.

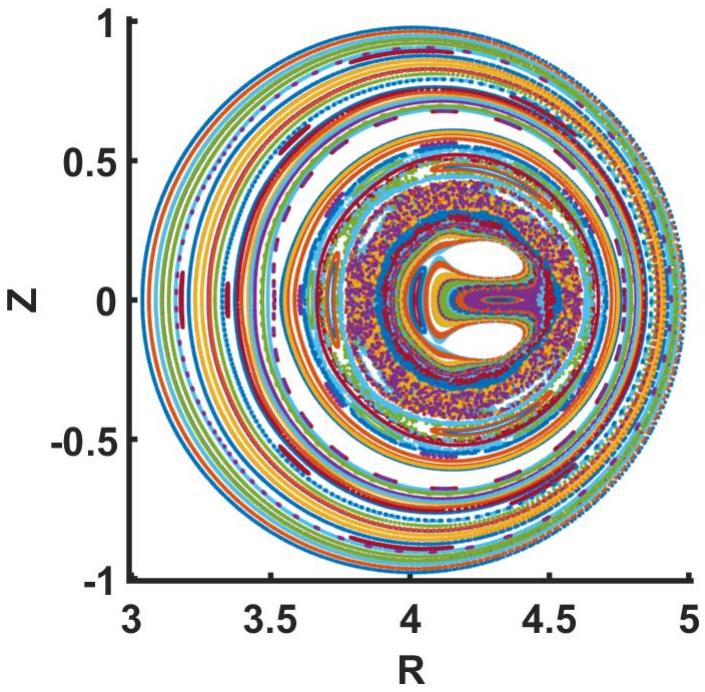

Figure 9 Poincare plots in the steady-state of sawtooth oscillations with low viscosity (ν_0=6.0×10^{-6}).

When we choose an extremely high viscosity, ν_0=1.0×10^{-3}, it is found that the oscillation could also gradually evolves into a steady-state, as shown in Figure 10 and Figure 11. The kinetic energy and the pressure profiles remain almost unchanged after $t = 25000t_A$. The Poincare plots of the magnetic field at the steady-state stage is shown in Figure 12.

From the simulation results given in the subsection, it indicates that the system can both turn into the steady-state with relatively high or low viscosity. The normal sawtooth oscillation can only take place in the intermediate viscosity regime.

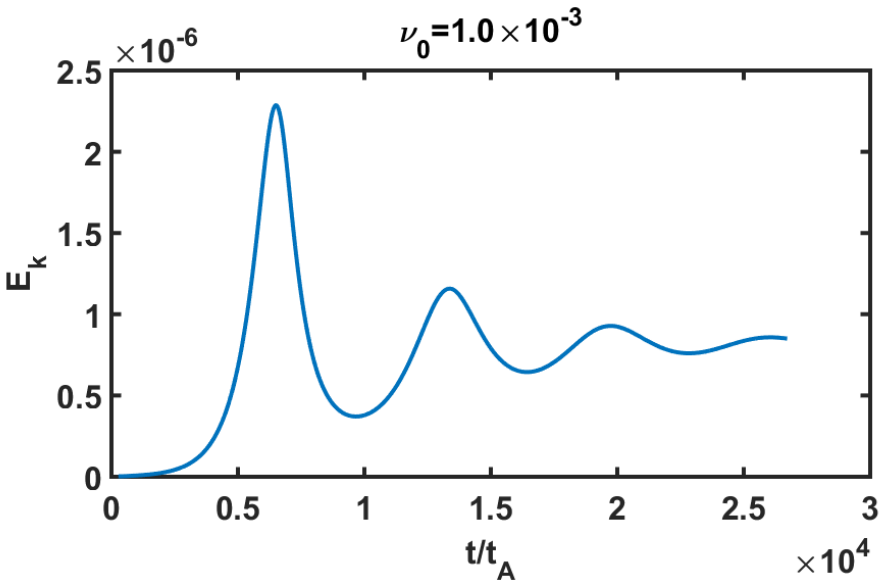

Figure 10 Evolution of the kinetic energy with $\nu_0=1.0\times10^{-3}$. After several cycles, the system eventually evolves into a stationary state and the kinetic energy almost remains unchanged after $t=25000t_A$.

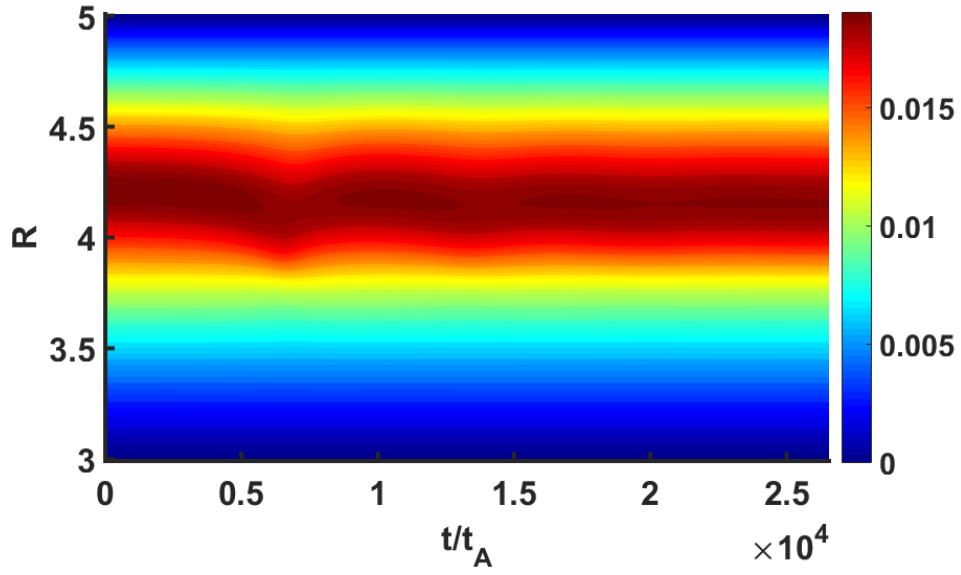

Figure 11 Evolution of the pressure profile at Z=0 with $\nu_0=1.0\times10^{-3}$. After $t=25000t_A$, the pressure profile almost remains unchanged.

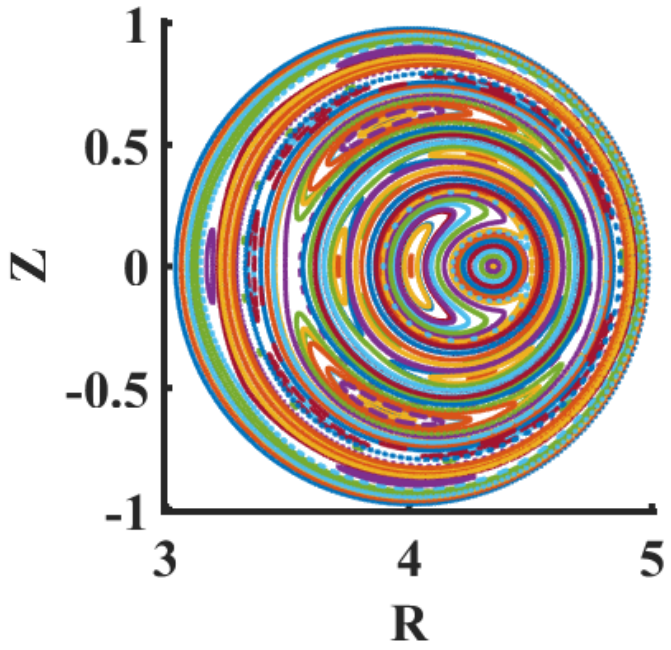

Figure 12 Poincare plots in the steady-state of sawtooth oscillations with high viscosity (ν_0=1.0×10^{-3}).

B. Sawtooth oscillations with low β

It should be noted that Shen et al. [29] only presented the sawtooth behavior in the regime of the viscosity $\upsilon \geq 1.0\times10^{-5}$ with a low plasma beta, $\beta = 0.2\%$. Their results indicate that the system exhibits a normal sawtooth oscillation with the lower viscosity while the sawtooth eventually evolves into a steady-state with the higher viscosity. Therefore, we carry out a series of simulations with a broader parameter regime of the viscosity and the same plasma beta, $\beta = 0.2\%$ to check whether the system could turn into the steady-state with sufficient low viscosity. Other parameters and the initial profiles are the same as in Section III. A. The evolutions of the kinetic energy with $\upsilon = 1.0\times10^{-3}$, $\upsilon = 1.0\times10^{-4}$, $\upsilon = 1.0\times10^{-5}$, and $\upsilon = 1.0\times10^{-6}$ are shown in Figure 13. With $\upsilon = 1.0\times10^{-3}$, the oscillation evolves into a steady-state after serval oscillations, and it remains the normal sawtooth with $\upsilon = 1.0\times10^{-4}$ or $\upsilon = 1.0\times10^{-5}$, which is similar to the Figure 10 in Ref. [29]. It is interestingly noted

that with sufficient low viscosity ($\upsilon = 1.0\times10^{-6}$), the system can also turn into the steady-state, which is not presented in Ref. [29].

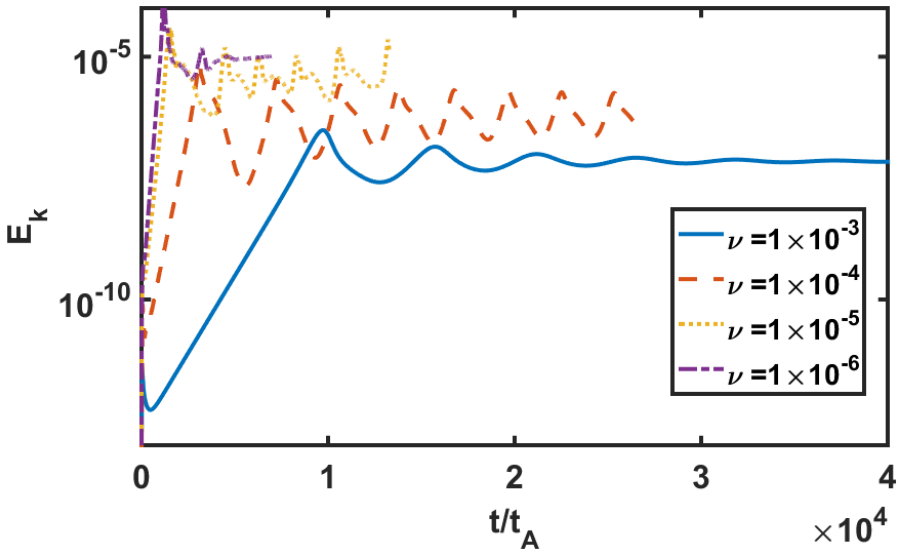

Figure 13 Evolutions of the kinetic energy with $\upsilon = 1.0\times10^{-3}$, $\upsilon = 1.0\times10^{-4}$, $\upsilon = 1.0\times10^{-5}$ and $\upsilon = 1.0\times10^{-6}$.

C. β scanning

From Subsection III. A and B, the middle parameter regime for the normal sawtooth is broadened when the plasma beta is lower. Therefore, we systematically investigate the influence of β on dynamics of the sawtooth oscillations. The long-time behaviors of the sawtooth oscillation with different β and viscosity are shown in Figure 14. The normal sawtooth oscillations are labeled with blue diamonds. Since the small sawtooth oscillations reach a steady-state after serval cycles, we label both small sawtooth oscillations and steady-states with red squares. As shown in Figure 14, the normal sawtooth only occurs with intermediate viscosity while the small sawtooth or the steady-state happen with high viscosity ($\upsilon \geq 1.0\times10^{-3}$) or low viscosity regime ($\upsilon \leq 1.0\times10^{-5}$). It is obvious that the steady-state discussed in Ref. [29] is just the steady-state in the high viscosity regime.

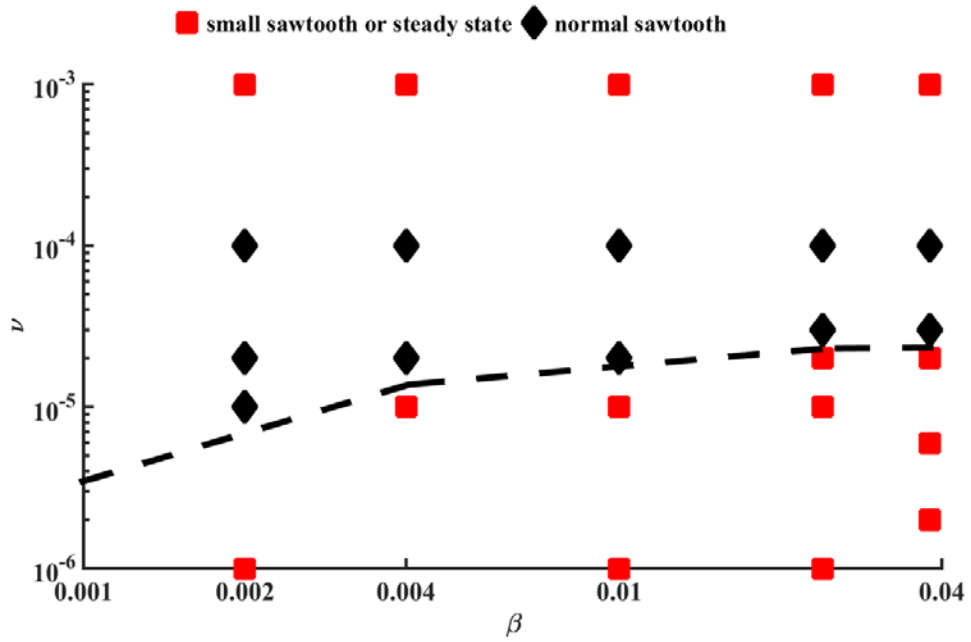

Figure 14 Long-time behavior of sawtooth oscillations with different β and viscosity.

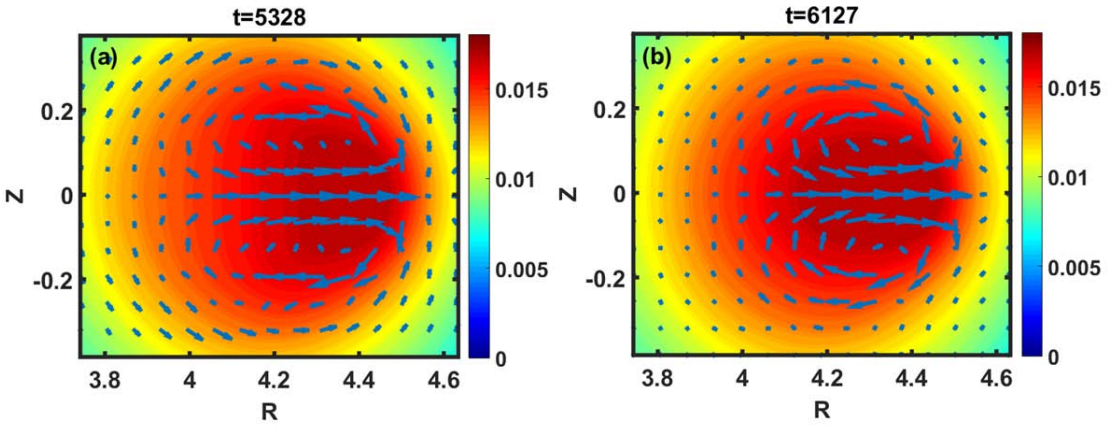

Figure 15 Flow patterns (the arrows) and pressure distributions (the contour plot) at (a) $t = 5328t_A$ just before the crash and (b) $t = 6127t_A$ after the crash for a small sawtooth. The flow is not entirely damped out at the end of the small sawtooth cycle. All the vectors are normalized by the maximum velocity in (a).

D. Physical reasons for achieve the second type of steady-state

From the discussions above, we know that the behavior of the system will be (a) a steady-state with extremely high viscosity, (b) a normal sawtooth with medium viscosity, (c) small sawtooth oscillations with lower viscosity, and (d) a steady-state

with sufficient low viscosity. The steady-state with extremely high viscosity is easy to understand- the system is stuck since the viscosity is extremely high. However, why could the system reach a steady-state with a sufficient low viscosity?

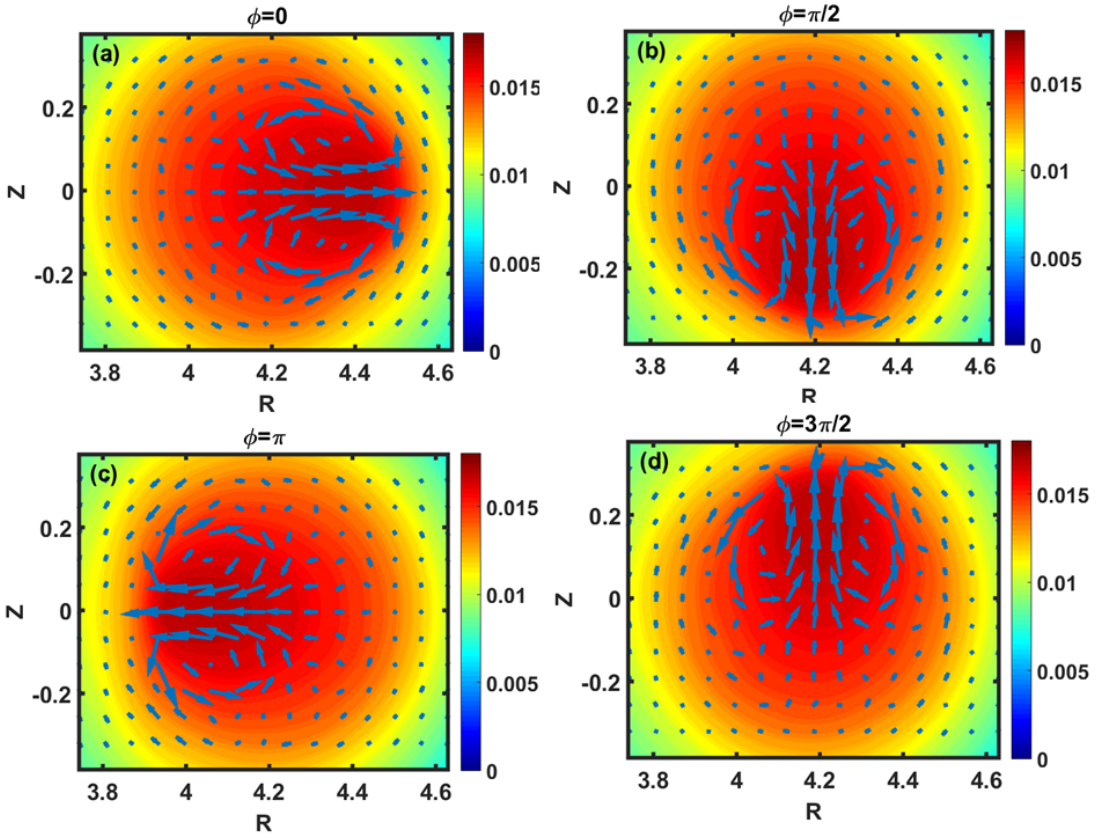

Figure 16 Flow patterns of the stationary state at ϕ=0, ϕ=π/2, ϕ=π and ϕ=3π/2, respectively. All the vectors are normalized by the maximum velocity during the simulations of the steady-state. It is evident that there exists a strong residual flow with m/n=1/1 helicity at the steady-state.

From the evolutions of kinetic energy Figure 2, Figure 4 and Figure 7, there exists a remarkable difference in the three kinds of sawtooth- the residual flow after each sawtooth cycle. As shown in Figure 2, there is no residual flow since the kinetic energy is almost zero after each cycle. For the small sawtooth oscillations and the second type steady-state, the residual flow is notable (Figure 15 and Figure 16). It should be noted that, the magnetic flux is frozen in the plasma except for the reconnection region. Since the direction of the residual flow is from the core to the reconnection region, it continuously carries magnetic flux into the reconnection region due to the frozen in condition. It also should be noted that, in our model, the

new pumped magnetic flux is mainly due to the dynamo effect in the Ohm's Law (Eq. 5). Since the toroidal current is significantly reduced from the initial value, new magnetic flux is continuously pumped in the core region. The reason for the system reaching a steady-state is the balance between the new pumped magnetic flux in the core region and the flux loss in the reconnection region and the 'bridge' is the residual flow. The current profiles for the initial equilibrium and two types of steady-state are shown in Figure 17, which could clearly indicate the mechanism for the steady-state, i. e. a dynamo in the core region, a thin and sharp current sheet at the resonant surface, and a strong residual flow (Figure 16).

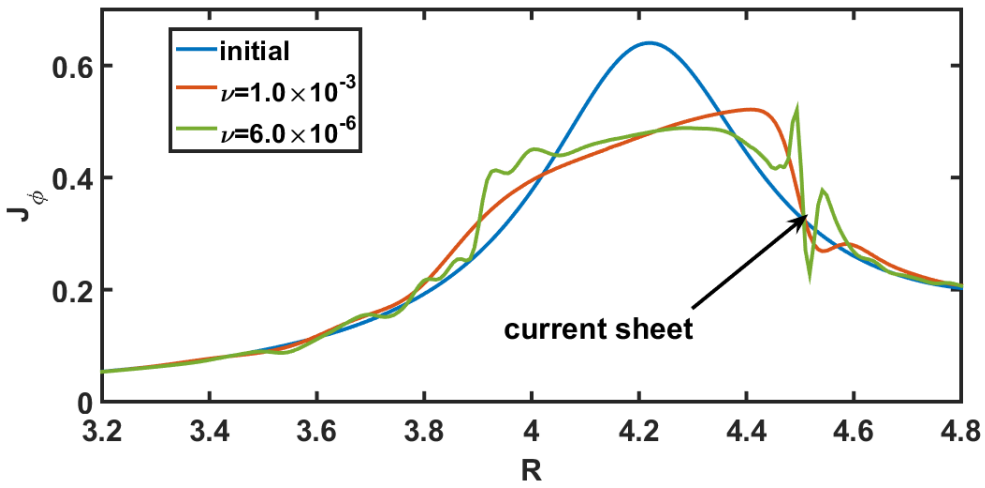

Figure 17 The current profiles for the initial equilibrium and two types of steady-state.

It also should be noted that the intermediate regime of the viscosity for the normal sawtooth becomes border with decreasing plasma beta (Figure 14). The lower boundary of the intermediate regime increases from $\upsilon = 1.0\times10^{-6}$ for the low β cases to $\upsilon = 2.0\times10^{-5}$ for the high β cases. The reason is that the lower β, the lower residual flow (Figure 18), and then lower viscosity is needed for achieving the steady-state.

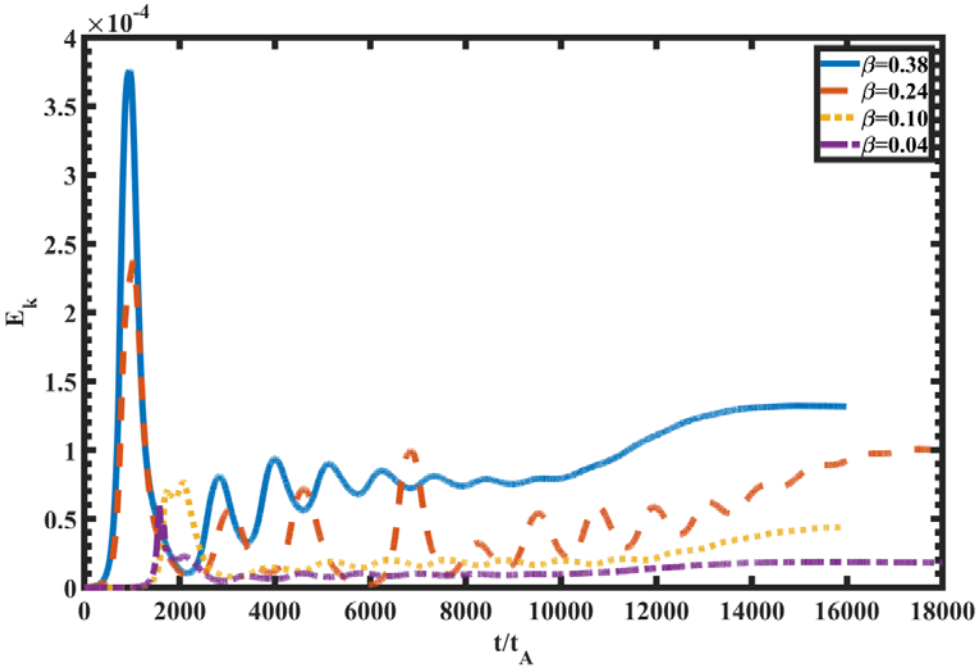

Figure 18 Kinetic energy evolutions with $\upsilon = 1.0 \times 10^{-5}$ and different β.

IV. Discussion

A systematical simulation study is conducted to investigate the influence of viscosity and plasma beta on dynamics of sawtooth oscillations. It is found that there are two parameter regimes of the viscosity for achieving the steady-state of the sawtooth oscillations. With sufficient high or low viscosity, the system eventually evolves into a small sawtooth oscillation or a quasi-steady state. In the intermediate viscosity, it becomes a normal sawtooth.

With sufficient low viscosity, the residual flow after each sawtooth cycle could be sufficient strong. Due to the frozen in condition, the residual flow could continuously transfer the magnetic flux in the core region to the reconnection region. Then a balance between the new magnetic flux pumped by the dynamo effect in the core region and magnetic flux loss in the reconnection region.

It is also found that the transition viscosity between the normal sawtooth and the small sawtooth or the steady-state increases with increasing β. It is because the residual flow increases with increasing β, and a higher viscosity is needed to

suppress the residual flow.

It should be noted that, although a steady-state could be achieved in the parameter regime of high viscosity and low beta in the numerical simulations, it is unlikely relevant to present Tokamaks, since the plasma beta is high and the viscosity is low in modern Tokamaks. However, the steady-state in the low viscosity and the high plasma beta regime might be related to the stationary state observed in present Tokamaks.[37, 44, 45] In the steady-state, the mode structure is non-axisymmetric with the m/n=1/1 helicity.

Acknowledgment

One of the authors (W. Zhang) would like to thank Dr. S. C. Jardin for his useful comments. This work is supported by the National Natural Science Foundation of China under Grant No. 11775188 and 11835010, the Special Project on High-performance Computing under the National Key R&D Program of China No. 2016YFB0200603, Fundamental Research Fund for Chinese Central Universities.

[1] S. von Goeler, W. Stodiek, N. Sauthoff, Studies of Internal Disruptions and $m=1$ Oscillations in Tokamak Discharges with Soft\char22{}X-Ray Tecniques, Physical Review Letters, 33 (1974) 1201-1203.

[2] K. McGuire, D.C. Robinson, Sawtooth oscillations in a small tokamak, Nuclear Fusion, 19 (1979) 505.

[3] M.A. Dubois, A.L. Pecquet, C. Reverdin, Internal disruptions in the TFR tokamak: A phenomenological analysis, Nuclear Fusion, 23 (1983) 147.

[4] T.C. Hender, J.C. Wesley, J. Bialek, A. Bondeson, A.H. Boozer, R.J. Buttery, A. Garofalo, T.P. Goodman, R.S. Granetz, Y. Gribov, O. Gruber, M. Gryaznevich, G. Giruzzi, S. Günter, N. Hayashi, P. Helander, C.C. Hegna, D.F. Howell, D.A. Humphreys, G.T.A. Huysmans, A.W. Hyatt, A. Isayama, S.C. Jardin, Y. Kawano, A. Kellman, C. Kessel, H.R. Koslowski, R.J.L. Haye, E. Lazzaro, Y.Q. Liu, V. Lukash, J. Manickam, S. Medvedev, V. Mertens, S.V. Mirnov, Y. Nakamura, G. Navratil, M. Okabayashi, T. Ozeki, R. Paccagnella, G. Pautasso, F. Porcelli, V.D. Pustovitov, V. Riccardo, M. Sato, O. Sauter, M.J. Schaffer, M. Shimada, P. Sonato, E.J. Strait, M. Sugihara, M. Takechi, A.D. Turnbull, E. Westerhof, D.G. Whyte, R. Yoshino, H. Zohm, D. the Itpa Mhd, G. Magnetic Control Topical, Chapter 3: MHD stability, operational limits and disruptions, Nuclear Fusion, 47 (2007) S128.

[5] A. Letsch, H. Zohm, F. Ryter, W. Suttrop, A. Gude, F. Porcelli, C. Angioni, I. Furno, Incomplete reconnection in sawtooth crashes in ASDEX Upgrade, Nuclear Fusion, 42 (2002) 1055.

[6] I. Furno, C. Angioni, F. Porcelli, H. Weisen, R. Behn, T.P. Goodman, M.A. Henderson, Z.A. Pietrzyk, A. Pochelon, H. Reimerdes, E. Rossi, Understanding sawtooth activity during intense electron cyclotron heating experiments on TCV, Nuclear Fusion, 41 (2001) 403.

[7] A.W. Edwards, D.J. Campbell, W.W. Engelhardt, H.U. Fahrbach, R.D. Gill, R.S. Granetz, S. Tsuji, B.J.D. Tubbing, A. Weller, J. Wesson, D. Zasche, Rapid Collapse of a Plasma Sawtooth Oscillation in the JET Tokamak, Physical Review Letters, 57 (1986) 210-213.
[8] K. McGuire, V. Arunasalam, C.W. Barnes, M.G. Bell, M. Bitter, R. Boivin, N.L. Bretz, R. Budny, C.E. Bush, A. Cavallo, T.K. Chu, S.A. Cohen, P. Colestock, S.L. Davis, D.L. Dimock, H.F. Dylla, P.C. Efthimion, A.B. Ehrhrardt, R.J. Fonck, E. Fredrickson, H.P. Furth, G. Gammel, R.J. Goldston, G. Greene, B. Grek, L.R. Grisham, G. Hammett, R.J. Hawryluk, H.W. Hendel, K.W. Hill, E. Hinnov, D.J. Hoffman, J. Hosea, R.B. Howell, H. Hsuan, R.A. Hulse, A.C. Janos, D. Jassby, F. Jobes, D.W. Johnson, L.C. Johnson, R. Kaita, C. Kieras‐Phillips, S.J. Kilpatrick, P.H. LaMarche, B. LeBlanc, D.M. Manos, D.K. Mansfield, E. Mazzucato, M.P. McCarthy, M.C. McCune, D.H. McNeill, D.M. Meade, S.S. Medley, D.R. Mikkelsen, D. Monticello, R. Motley, D. Mueller, J.A. Murphy, Y. Nagayama, D.R. Nazakian, E.B. Neischmidt, D.K. Owens, H. Park, W. Park, S. Pitcher, A.T. Ramsey, M.H. Redi, A.L. Roquemore, P.H. Rutherford, G. Schilling, J. Schivell, G.L. Schmidt, S.D. Scott, J.C. Sinnis, J. Stevens, B.C. Stratton, W. Stodiek, E.J. Synakowski, W.M. Tang, G. Taylor, J.R. Timberlake, H.H. Towner, M. Ulrickson, S.v. Goeler, R. Wieland, M. Williams, J.R. Wilson, K.L. Wong, M. Yamada, S. Yoshikawa, K.M. Young, M.C. Zarnstorff, S.J. Zweben, High‐beta operation and magnetohydrodynamic activity on the TFTR tokamak, Physics of Fluids B: Plasma Physics, 2 (1990) 1287-1290.
[9] D.J. Campbell, R.D. Gill, C.W. Gowers, J.A. Wesson, D.V. Bartlett, C.H. Best, S. Coda, A.E. Costley, A. Edwards, S.E. Kissel, R.M. Niestadt, H.W. Piekaar, R. Prentice, R.T. Ross, B.J.D. Tubbing, Sawtooth activity in ohmically heated JET plasmas, Nuclear Fusion, 26 (1986) 1085-1092.
[10] O. Sauter, E. Westerhof, M.L. Mayoral, B. Alper, P.A. Belo, R.J. Buttery, A. Gondhalekar, T. Hellsten, T.C. Hender, D.F. Howell, T. Johnson, P. Lamalle, M.J. Mantsinen, F. Milani, M.F.F. Nave, F. Nguyen, A.L. Pecquet, S.D. Pinches, S. Podda, J. Rapp, Control of Neoclassical Tearing Modes by Sawtooth Control, Physical Review Letters, 88 (2002) 105001.
[11] R.J. Buttery, T.C. Hender, D.F. Howell, R.J.L. Haye, O. Sauter, D. Testa, Onset of neoclassical tearing modes on JET, Nuclear Fusion, 43 (2003) 69.
[12] D.J. Campbell, D.F.H. Start, J.A. Wesson, D.V. Bartlett, V.P. Bhatnagar, M. Bures, J.G. Cordey, G.A. Cottrell, P.A. Dupperex, A.W. Edwards, C.D. Challis, C. Gormezano, C.W. Gowers, R.S. Granetz, J.H. Hammen, T. Hellsten, J. Jacquinot, E. Lazzaro, P.J. Lomas, N.L. Cardozo, P. Mantica, J.A. Snipes, D. Stork, P.E. Stott, P.R. Thomas, E. Thompson, K. Thomsen, G. Tonetti, Stabilization of Sawteeth with Additional Heating in the JET Tokamak, Physical Review Letters, 60 (1988) 2148-2151.
[13] R.J. Buttery, T.C. Hender, D.F. Howell, R.J.L. Haye, S. Parris, O. Sauter, C.G. Windsor, J.-E. Contributors, On the form of NTM onset scalings, Nuclear Fusion, 44 (2004) 678.
[14] I.T. Chapman, Controlling sawtooth oscillations in tokamak plasmas, Plasma Physics and Controlled Fusion, 53 (2011) 013001.
[15] M. Shimada, D.J. Campbell, V. Mukhovatov, M. Fujiwara, N. Kirneva, K. Lackner, M. Nagami, V.D. Pustovitov, N. Uckan, J. Wesley, N. Asakura, A.E. Costley, A.J.H. Donné, E.J. Doyle, A. Fasoli, C. Gormezano, Y. Gribov, O. Gruber, T.C. Hender, W. Houlberg, S. Ide, Y. Kamada, A. Leonard, B. Lipschultz, A. Loarte, K. Miyamoto, V. Mukhovatov, T.H. Osborne, A. Polevoi, A.C.C. Sips, Chapter 1: Overview and summary, Nuclear Fusion, 47 (2007) S1.
[16] G.H. Choe, G.S. Yun, H.K. Park, J.H. Jeong, Slow crash in modified sawtooth patterns driven by localized electron cyclotron heating and current drive in KSTAR, Nuclear Fusion, 58 (2018) 106038.
[17] M. Sertoli, T. Odstrcil, C. Angioni, A.U.T. the, Interplay between central ECRH and saturated (m , n) = (1, 1) MHD activity in mitigating tungsten accumulation at ASDEX Upgrade, Nuclear Fusion, 55

(2015) 113029.
[18] Z.Y. Cui, K. Zhang, S. Morita, X.Q. Ji, X.T. Ding, Y. Xu, P. Sun, J.M. Gao, C.F. Dong, D.L. Zheng, Y.G. Li, M. Jiang, D. Li, W.L. Zhong, L. Yi, Y.B. Dong, S.D. Song, L.M. Yu, Z.B. Shi, B.Z. Fu, P. Lu, M. Huang, B.S. Yuan, Q.W. Yang, X.R. Duan, Study of impurity transport in HL-2A ECRH L-mode plasmas with radially different ECRH power depositions, Nuclear Fusion, 58 (2018) 056012.
[19] E. Li, V. Igochine, O. Dumbrajs, L. Xu, K. Chen, T. Shi, L. Hu, The non-resonant kink modes triggering strong sawtooth-like crashes in the EAST tokamak, Plasma Physics and Controlled Fusion, 56 (2014) 125016.
[20] T. team, H.K. Park, N.C. Luhmann, A.J.H. Donné, I.G.J. Classen, C.W. Domier, E. Mazzucato, T. Munsat, M.J. van de Pol, Z. Xia, Observation of High-Field-Side Crash and Heat Transfer during Sawtooth Oscillation in Magnetically Confined Plasmas, Physical Review Letters, 96 (2006) 195003.
[21] Y. Sun, B. Wan, L. Hu, B. Shen, Understanding the m = 1 mode during the sawtooth ramp phase in lower hybrid current driven plasmas on the HT-7 tokamak, Nuclear Fusion, 47 (2007) 271.
[22] J.P. Graves, I.T. Chapman, S. Coda, M. Lennholm, M. Albergante, M. Jucker, Control of magnetohydrodynamic stability by phase space engineering of energetic ions in tokamak plasmas, Nature Communications, 3 (2012) 624.
[23] E. Lerche, M. Lennholm, I.S. Carvalho, P. Dumortier, F. Durodie, D.V. Eester, J. Graves, P. Jacquet, A. Murari, J.E.T. Contributors, Sawtooth pacing with on-axis ICRH modulation in JET-ILW, Nuclear Fusion, 57 (2017) 036027.
[24] D. Kim, T.P. Goodman, O. Sauter, Real-time sawtooth control and neoclassical tearing mode preemption in ITER, Physics of Plasmas, 21 (2014) 061503.
[25] Z. Chen, M. Nocente, M. Tardocchi, T. Fan, G. Gorini, Simulation of neutron emission spectra from neutral beam-heated plasmas in the EAST tokamak, Nuclear Fusion, 53 (2013) 063023.
[26] C.C. Petty, M.E. Austin, C.T. Holcomb, R.J. Jayakumar, R.J. La Haye, T.C. Luce, M.A. Makowski, P.A. Politzer, M.R. Wade, Magnetic-Flux Pumping in High-Performance, Stationary Plasmas with Tearing Modes, Physical Review Letters, 102 (2009) 045005.
[27] S.C. Jardin, N. Ferraro, I. Krebs, Self-Organized Stationary States of Tokamaks, Physical Review Letters, 115 (2015) 215001.
[28] I. Krebs, S.C. Jardin, S. Günter, K. Lackner, M. Hoelzl, E. Strumberger, N. Ferraro, Magnetic flux pumping in 3D nonlinear magnetohydrodynamic simulations, Physics of Plasmas, 24 (2017) 102511.
[29] W. Shen, F. Porcelli, Linear and nonlinear simulations of the visco-resistive internal kink mode using the M3D code, Nuclear Fusion, 58 (2018) 106035.
[30] O. Février, T. Nicolas, P. Maget, J.H. Ahn, X. Garbet, H. Lütjens, Non-linear MHD simulations of sawteeth and their control by current and power depositions, Nuclear Fusion, 58 (2018) 096008.
[31] J.-H. Ahn, X. Garbet, H. Lütjens, A. Marx, T. Nicolas, R. Sabot, J.-F. Luciani, R. Guirlet, O. Février, P. Maget, Non-linear dynamics of compound sawteeth in tokamaks, Physics of Plasmas, 23 (2016) 052509.
[32] D. Bonfiglio, M. Veranda, S. Cappello, L. Chacón, D.F. Escande, Sawtooth mitigation in 3D MHD tokamak modelling with applied magnetic perturbations, Plasma Physics and Controlled Fusion, 59 (2017) 014032.
[33] J.P. Graves, D. Brunetti, I.T. Chapman, W.A. Cooper, H. Reimerdes, F. Halpern, A. Pochelon, O. Sauter, Magnetohydrodynamic helical structures in nominally axisymmetric low-shear tokamak plasmas, Plasma Physics and Controlled Fusion, 55 (2012) 014005.
[34] L. Delgado-Aparicio, L. Sugiyama, R. Granetz, D.A. Gates, J.E. Rice, M.L. Reinke, M. Bitter, E.

Fredrickson, C. Gao, M. Greenwald, K. Hill, A. Hubbard, J.W. Hughes, E. Marmar, N. Pablant, Y. Podpaly, S. Scott, R. Wilson, S. Wolfe, S. Wukitch, Formation and Stability of Impurity ``Snakes'' in Tokamak Plasmas, Physical Review Letters, 110 (2013) 065006.
[35] J.A. Breslau, M.S. Chance, J. Chen, G.Y. Fu, S. Gerhardt, N. Gorelenkov, S.C. Jardin, J. Manickam, Onset and saturation of a non-resonant internal mode in NSTX and implications for AT modes in ITAB, Nuclear Fusion, 51 (2011) 063027.
[36] W.A. Cooper, J.P. Graves, O. Sauter, I.T. Chapman, M. Gobbin, L. Marrelli, P. Martin, I. Predebon, D. Terranova, Magnetohydrodynamic properties of nominally axisymmetric systems with 3D helical core, Plasma Physics and Controlled Fusion, 53 (2011) 074008.
[37] P. Buratti, M. Baruzzo, R.J. Buttery, C.D. Challis, I.T. Chapman, F. Crisanti, L. Figini, M. Gryaznevich, T.C. Hender, D.F. Howell, H. Han, F. Imbeaux, E. Joffrin, J. Hobirk, O.J. Kwon, X. Litaudon, J. Mailloux, J.-E. contributors, Kink instabilities in high-beta JET advanced scenarios, Nuclear Fusion, 52 (2012) 023006.
[38] F.D. Halpern, H. Lütjens, J.-F. Luciani, Diamagnetic thresholds for sawtooth cycling in tokamak plasmas, Physics of Plasmas, 18 (2011) 102501.
[39] F.D. Halpern, D. Leblond, H. Lütjens, J.F. Luciani, Oscillation regimes of the internal kink mode in tokamak plasmas, Plasma Physics and Controlled Fusion, 53 (2010) 015011.
[40] L. Delgado-Aparicio, L. Sugiyama, R. Granetz, D. Gates, J. Rice, M.L. Reinke, W. Bergerson, M. Bitter, D.L. Brower, E. Fredrickson, C. Gao, M. Greenwald, K. Hill, A. Hubbard, J. Irby, J.W. Hughes, E. Marmar, N. Pablant, S. Scott, R. Wilson, S. Wolfe, S. Wukitch, On the formation and stability of long-lived impurity-ion snakes in Alcator C-Mod, Nuclear Fusion, 53 (2013) 043019.
[41] R. Fischer, A. Bock, A. Burckhart, O.P. Ford, L. Giannone, V. Igochine, M. Weiland, M. Willensdorfer, Sawtooth induced q-profile evolution at ASDEX Upgrade, Nuclear Fusion, 59 (2019) 056010.
[42] E.A. Lazarus, T.C. Luce, M.E. Austin, D.P. Brennan, K.H. Burrell, M.S. Chu, J.R. Ferron, A.W. Hyatt, R.J. Jayakumar, L.L. Lao, J. Lohr, M.A. Makowski, T.H. Osborne, C.C. Petty, P.A. Politzer, R. Prater, T.L. Rhodes, J.T. Scoville, W.M. Solomon, E.J. Strait, A.D. Turnbull, F.L. Waelbroeck, C. Zhang, Sawtooth oscillations in shaped plasmas, Physics of Plasmas, 14 (2007) 055701.
[43] Y.B. Nam, J.S. Ko, G.H. Choe, Y. Bae, M.J. Choi, W. Lee, G.S. Yun, S. Jardin, H.K. Park, Validation of the ‘full reconnection model’ of the sawtooth instability in KSTAR, Nuclear Fusion, 58 (2018) 066009.
[44] I.T. Chapman, M.D. Hua, S.D. Pinches, R.J. Akers, A.R. Field, J.P. Graves, R.J. Hastie, C.A. Michael, Saturated ideal modes in advanced tokamak regimes in MAST, Nuclear Fusion, 50 (2010) 045007.
[45] N. Oyama, A. Isayama, G. Matsunaga, T. Suzuki, H. Takenaga, Y. Sakamoto, T. Nakano, Y. Kamada, S. Ide, Long-pulse hybrid scenario development in JT-60U, Nuclear Fusion, 49 (2009) 065026.
[46] S. Wang, Z. Ma, Influence of toroidal rotation on resistive tearing modes in tokamaks, Physics of Plasmas, 22 (2015) 122504.
[47] W. Zhang, S. Wang, Z.W. Ma, Influence of helical external driven current on nonlinear resistive tearing mode evolution and saturation in tokamaks, Physics of Plasmas, 24 (2017) 062510.
[48] W. Zhang, Z.W. Ma, S. Wang, Hall effect on tearing mode instabilities in tokamak, Physics of Plasmas, 24 (2017) 102510.
[49] W. Zhang, Z.W. Ma, H.W. Zhang, J. Zhu, Dynamic evolution of resistive kink mode with electron diamagnetic drift in tokamaks, Physics of Plasmas, 26 (2019) 042514.
[50] C. Cheng, M. Chance, NOVA: A nonvariational code for solving the MHD stability of axisymmetric toroidal plasmas, Journal of Computational Physics, 71 (1987) 124-146.
[51] A.Y. Aydemir, J.C. Wiley, D.W. Ross, Toroidal studies of sawtooth oscillations in tokamaks, Physics

of Fluids B: Plasma Physics, 1 (1989) 774-787.
[52] Q. Yu, S. Günter, K. Lackner, Numerical modelling of sawtooth crash using two-fluid equations, Nuclear Fusion, 55 (2015) 113008.
[53] A.C.C. Sips, R. Arslanbekov, C. Atanasiu, W. Becker, G. Becker, K. Behler, K. Behringer, A. Bergmann, R. Bilato, D. Bolshukhin, K. Borrass, B. Braams, M. Brambilla, F. Braun, A. Buhler, G. Conway, D. Coster, R. Drube, R. Dux, S. Egorov, T. Eich, K. Engelhardt, H.U. Fahrbach, U. Fantz, H. Faugel, M. Foley, K.B. Fournier, P. Franzen, J.C. Fuchs, J. Gafert, G. Gantenbein, O. Gehre, A. Geier, J. Gernhardt, O. Gruber, A. Gude, S. G nter, G. Haas, D. Hartmann, B. Heger, B. Heinemann, A. Herrmann, J. Hobirk, F. Hofmeister, H. Hohen cker, L. Horton, V. Igochine, D. Jacobi, M. Jakobi, F. Jenko, A. Kallenbach, O. Kardaun, M. Kaufmann, A. Keller, A. Kendl, J.W. Kim, K. Kirov, R. Kochergov, H. Kollotzek, W. Kraus, K. Krieger, B. Kurzan, P.T. Lang, P. Lauber, M. Laux, F. Leuterer, A. Lohs, A. Lorenz, C. Maggi, H. Maier, K. Mank, M.E. Manso, M. Maraschek, K.F. Mast, P. McCarthy, D. Meisel, H. Meister, F. Meo, R. Merkel, D. Merkl, V. Mertens, F. Monaco, A. M ck, H.W. M ller, M. M nich, H. Murmann, Y.S. Na, G. Neu, R. Neu, J. Neuhauser, J.M. Noterdaeme, I. Nunes, G. Pautasso, A.G. Peeters, G. Pereverzev, S. Pinches, E. Poli, M. Proschek, R. Pugno, E. Quigley, G. Raupp, T. Ribeiro, R. Riedl, S. Riondato, V. Rohde, J. Roth, F. Ryter, S. Saarelma, W. Sandmann, S. Schade, H.B. Schilling, W. Schneider, G. Schramm, S. Schweizer, B. Scott, U. Seidel, F. Serra, S. Sesnic, C. Sihler, A. Silva, E. Speth, A. St bler, K.H. Steuer, J. Stober, B. Streibl, E. Strumberger, W. Suttrop, A. Tabasso, A. Tanga, G. Tardini, C. Tichmann, W. Treutterer, M. Troppmann, P. Varela, O. Vollmer, D. Wagner, U. Wenzel, F. Wesner, R. Wolf, E. Wolfrum, E. W rsching, Q. Yu, D. Zasche, T. Zehetbauer, H.P. Zehrfeld, H. Zohm, Steady state advanced scenarios at ASDEX Upgrade, Plasma Physics and Controlled Fusion, 44 (2002) B69-B83.
[54] W.A. Cooper, J.P. Graves, A. Pochelon, O. Sauter, L. Villard, Tokamak Magnetohydrodynamic Equilibrium States with Axisymmetric Boundary and a 3D Helical Core, Physical Review Letters, 105 (2010) 035003.